UNIVNET 2022

Innovative Machines, Technologies and Materials
in Circular Economy Environment

PROCEEDINGS

September 26 - 28, 2022
Hotel Kaskada Brno, Czech Republic

UNIVNET 2022

Innovative Machines, Technologies and Materials
in Circular Economy Environment

CONFERENCE PROCEEDINGS

September 26 - 28, 2022
Hotel Kaskáda Brno, Czech Republic

Website: https://univnet.elfa.sk/

ISBN: 979-8-3503-9811-3
IEEE Catalog number: CFP22DL6-USB
Proceedings editor: Štefan Fejedelem

TABLE OF CONTENTS

Theoretical and practical aspects of the application of semiconductor ferroelectrics as energy-generating and energy-saving elements

A. Molnar*, V. Gerasimov**, D. Gal* and M. Badida***
* Uzhhorod National University, Department of the Physics of Semiconductors, Uzhhorod, Ukraine, alexander.molnar@uzhnu.edu.ua
** Mukachevo State University, Department of Engineering and PE, Mukachevo, Ukraine, vitgerv@gmail.com
*** Technical University of Kosice, Faculty of Mechanical Engineering, Kosice, Slovakia miroslav.badida@tuke.sk

***Abstract* — The article deals with the results of a study of 2D and 3D ferroelectrics as multifunctional converters of light, heat, motion, and deformation into electricity with their subsequent accumulation. A description of a prototype of a multifunctional generator based on CuInP2S6 and Sn2P2S6 crystals has been presented. A study of the parameters of crystals was carried out, as well as the results of their optimization to improve their characteristics.**

I. Introduction

Recently, in connection with the crisis of classical energy and the development of alternative one, developers of electronic devices are increasingly attaching importance to reducing the power consumption of modern electronic devices. Thanks to this trend, the power consumption of modern devices, such as microprocessors and microcontrollers, memory devices, analog microcircuits, etc. has decreased tenfold compared to a decade ago. This has led to the possibility of developing alternative micro-energy devices that allow the creation of self-powered ones with virtually unlimited service life. This has become especially relevant with the introduction of the so-called Internet of things (IoT), smart toothbrushes, wheels, clothes, etc. into our daily lives. They can be powered by mechanical movement, deformation, heat or lighting. These devices use different physical effects, such as photovoltaic, piezoelectric, pyroelectric or triboelectric effects. Most micro converters are based on one of the above phenomena, however, functional devices that are capable of using several effects simultaneously are more promising. One of the most interesting materials for modern functional electronics is ferroelectrics [1] which can simultaneously use at least 3-4 of the listed physical effects (Figure. 1). Many articles and books have recently been devoted to the prospects and possibilities of their application in the field of alternative micro-energy [2-10]. However, before real serial devices, there is still a lot of work to be done on the choice of suitable materials, engineering of complete solutions with low cost and a wide range of applicable parameters. We have developed an alternative microgenerator based on $CuInP_2S_6$ layered crystals and $Sn_2P_2S_6$ 3D crystal which is capable of simultaneously converting deformation, movement or vibration as well as changes in heat and lighting into electric current and with wide scaling capabilities (from tenths of millimeters to square meters).

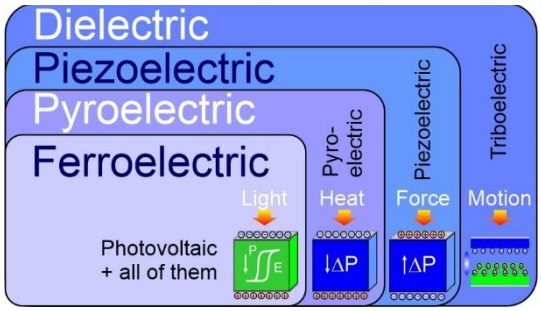

Figure 1. Dielectric, piezoelectric, pyroelectric, and ferroelectric material relationships and physical effects in them that can be used to generate electricity.

II. Transducer Material Selection

In most practical developments based on ferroelectrics, oxide crystals, ceramics or composites are used. This is due to their manufacturability, wide operating temperature range and good stability. However, as devices are reduced in size, there is a limitation due to the size effect which complicates the creation of devices smaller than 50 microns. Interface problems also arise when it is necessary to combine them with other materials of electronic engineering, especially two-dimensional ones, such as graphene. Therefore, in recent years, it has become relevant to use materials of the type $Me^1Me^2P_2S(Se)_6$ or $Me_2P_2S(Se)_6$ [11], Figure 2. This class includes both 3D crystals of the type $(Pb_ySn_{1-y})_2P_2(Se_xS_{1-x})_6$ [13], layered 2D crystals $CuInP_2(Se_xS_{1-x})_6$, $CuCrP_2S_6$, $CuBiP_2Se_6$ and others, as well as 1D needle crystals $Cs_2Ag_2P_2Se_6$. From a practical point of view, sulfides are of greater interest, because of the phase transition temperatures in selenide compounds are in the low-temperature region. 3D crystals $Sn_2P_2S_6$ can be used as an active medium in nonlinear optical devices [14], in piezoelectric transducers and sensors [15,16], in pyroelectric devices [17,18], as a matrix for solid electrolytes [19], and others. Based on layered $CuInP_2S_6$ crystals, the main components of electronic devices have already been created, starting with diodes and transistors [20] and ending with memory cells [21]. To date, this material is the only ferroelectric in which, at room temperature, it was possible to observe stable polarization switching in a sample with a thickness of 4 nm [22]. In addition, similar crystals (for example, $Li_2FeP_2S_6$,

$Li_2NiP_2S_6$) are candidates for creating solid-state batteries with ultra-high capacity [23,24].

Among them, the most interesting are layered van-der-Waals crystals, for which there is the possibility of easy delamination by both mechanical and chemical methods, with the prospect of creating nanometer-sized devices consisting of one or two structural layers of the material. In addition, intercalation, the introduction of various chemical compounds into the van-der-Waals interlayer space, can be easily implemented in such crystals, which allows them to be used as a matrix for creating batteries or supercapacitors to store the generated electricity. In addition, the layered structure of such crystals makes it easy to combine them both, to create heterostructures and with existing and promising functional materials of modern electronics such as graphene, MoS_2, silicon, etc.

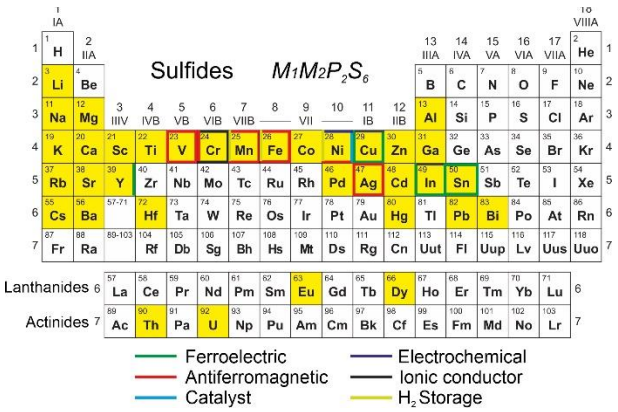

Figure 2. Functional properties of compounds in metal-phosphorus-chalcogen systems. Filled blocks represent elements for which the $M^1M^2P_2S_6$ structure has been reported to form (based on [11, 12] and our data).

$CuInP_2S_6$ crystals are an unusual example of a collinear ferroelectric system and illustrate the general features of cooperative dipole effects in layered chalcogen phosphates [25]. $CuInP_2S_6$ is a ferroelectric at $T < T_c = 315$ K (monoclinic spatial group *Cc*) because it contains polar lattices of Cu^I and In^{III} that are shifted in antiparallel directions relative to the median plane and detects spontaneous polarization $P_S = 3.5 - 4$ μC/cm^2 in the direction, perpendicular to the layer. The latter circumstance is very important for practical use since it does not require orientation of the samples before use (as in the case of 3D ferroelectrics $Sn_2P_2S_6$, as shown in our previous work [1], where the orientation of crystallites in an external electric field is required) and it is enough only to apply electrodes to its upper and lower planes, and the converter of illumination, temperature changes and deformation into electric current is ready. This crystal belongs to the group of "weak" ferroelectrics, the so-called ferroelectrics with the value of the coercive being 70 kV/cm. Besides, $CuInP_2S_6$ crystals are wide-gap semiconductors with a band gap E_g=2.8 eV, which has a positive effect on its photovoltaic properties and as shown in [25], they have an ionic component of the conductivity.

To create the generator, we used single crystals of $CuInP_2S_6$ obtained by the method of directed crystallization from the melt according to the method described in the work [26]. The resulting crystals were large, from which plates with an area of 1 cm^2 and a thickness of 0.5 mm were cut. As can be seen in the Figure 3, depending on the cooling rate and the purity of the initial components, the quality of the obtained crystals can differ significantly.

TABLE 1.
PARAMETERS FOR OBTAINING $CuInP_2S_6$ SINGLE CRYSTALS

Parameter	Value
The temperature of the melting zone	1150 K
The temperature of the annealing zone	870 K
Temperature gradient in the crystallization zone	3 K/mm
The crystallization front movement speed	2.5 mm/day
Cooling rate of the obtained crystal	200 K/day

The process was carried out in two-zone furnaces, and the temperature of the zones was regulated by using RIF-101 devices. The main technological parameters of the production process are given in Table 1.

The synthesis of the starting material was carried out by a two-temperature method from elementary components of high purity, taken in stoichiometric quantities directly in growth quartz ampoules, and pumped up to 0.013 Pa. The ampoule had a cylindrical "spout" with a length of 20 mm and an inner diameter of 4 mm for the formation of a monocrystalline seed.

As a result, monolithic $CuInP_2S_6$ boules with a diameter of 14 mm and a length of 20-25 mm (cylindrical part) with a well-developed cleavage were obtained, which makes it possible to easily manufacture samples of different thicknesses (Fig. 3). It should be noted that the optical characteristics of the obtained crystals slightly changed along the length.

Compared to crystals obtained from the gas phase, these samples are much larger (both in area and thickness), which provides an easier and cheaper way to create large-size transducers.

Figure 3. Single crystals of $CuInP_2S_6$ grown from a melt of different quality

The chemical composition of all grown and further investigated crystals was confirmed using TESCAN MIRA 3 Scanning Electron Microscope with EDAX EDS.

III. Experimental Setup

The photovoltaic characteristics of the studied samples were measured using LED light sources produced by Thorlabs: M505L3 (505 nm), M660L4 (660 nm), M810L3 (810 nm), and M940L3 (940 nm). The Thorlabs PM100 High Sensitivity Optical Power Meter was used to measure the illumination level with the S120B (Si) sensor, which works in the wavelength range of 400-1100 nm and power range of 50 nW to 50 mW. The output photovoltage level was fixed using OWON XDM 3041 digital multimeter.

The temperature dependence of permittivity and losses were measured using an automated measuring system [27] based on an LCR-819 impedance meter. To measure the temperature, we used the LabVIEW controlled Measurement Computing USB-TEMP-AI data acquisition device. As a temperature sensor, the PT100/1509A platinum thermistor of TDI Ltd. company (England) was applied. The temperature measurement accuracy was ±0.01 K. The heater power was changed using a Linear Programmable DC Power Supply OWON ODP3033.

IV. Photoelectric Properties

To study the photovoltaic characteristics, we used a $CuInP_2S_6$ crystal, obtained from the melt by the method of directed crystallization, with a size of 10x10 mm^2 and a thickness of 0.5 mm.

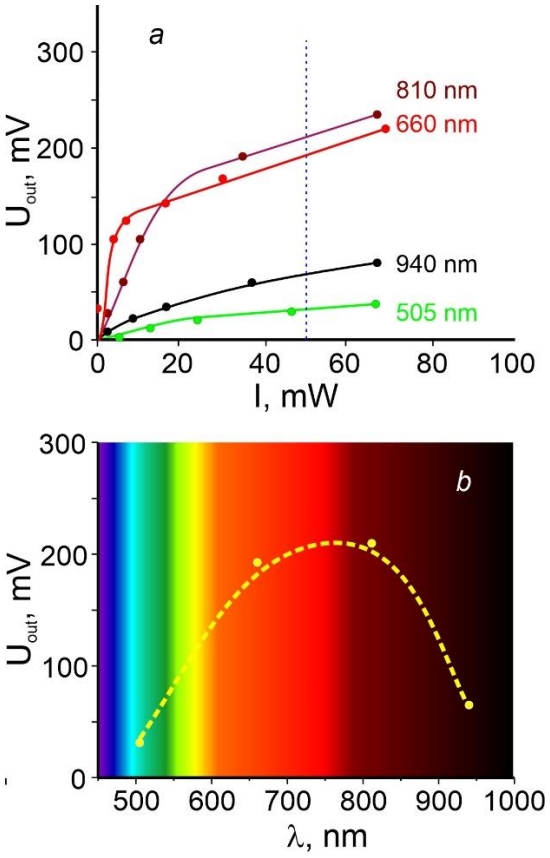

Figure 4. The dependence of the output voltage of the converter on the intensity of illumination - *a*. *b* - spectral sensitivity of the transducer at an illumination power of 50 mW.

An aluminum plate was used as the lower electrode to which the crystal was glued with a silver paste. We used a semitransparent vacuum deposited SnO electrode as the top electrode.

As we can see in Figure 4(*a*), with an increase in the illumination level, the initial, highly non-linear dependence of the output voltage, above 20 mW, goes into a more linear mode. The initial nonlinearity may be due to the presence of blocking space charges in the near-electrode regions.

As for the spectral characteristics of the photosensitivity (Figure 4(*b*)), it strongly resembles the behavior of $CuInP_2S_6$ crystals, which is not surprising, based on the close values of the band gap of both crystals (for $CuInP_2S_6$, $E_g \approx 2.8$ eV, and $E_g = 2.5$ eV for $Sn_2P_2S_6$). True, it should be noted the higher photosensitivity of $CuInP_2S_6$ crystals, which is two to three times higher than in the case of $Sn_2P_2S_6$ [1]. The maximum photosensitivity falls in the near- infrared range with a wavelength of 800 nm, which is most likely due to the depth of penetration of radiation into the bulk of the crystal. Based on this, it is possible to experimentally find the optimal thickness of the photosensitive layer for each wavelength.

V. Increasing the Phase Transition Temperature of $CuInP_2S_6$ Crystals

One of the significant drawbacks of the $CuInP_2S_6$ crystal is the relatively low phase transition temperature, which as noted earlier, is slightly more than 40 degrees Celsius. In the case of practical application this parameter is a significant limiting factor. For example, when using them as photoconverters or pyroelectric converters, due to heating, the crystal can easily overheat, passing into the paraelectric phase, and losing its ferroelectric properties. In this regard, the search for ways to increase the phase transition temperature of $CuInP_2S_6$ crystals remains very relevant. At the moment, there are two ways to increase the phase transition temperature of $CuInP_2S_6$ samples. This is a uniaxial or hydrostatic compression of crystals (which is very difficult to implement in practice) [29] or a change in the chemical composition of the material [30]. We went the second way.

When studying the dielectric properties of $CuInP_2S_6$ crystals, it was established that both the phase transition temperature and some properties of the crystals change significantly from batch to batch. This is obviously due to the deviation from stoichiometry. The most likely reason for this phenomenon is probably to be a large difference in the rate of mass transfer of copper and indium. Therefore, in order to optimize the properties of these crystals, we studied samples that were grown by the chemical transport reaction (CTR) method, both from a charge with a stoichiometric composition and a composition of $0.9{\cdot}CuInP_2S_6$ - $0.1{\cdot}Cu_2S$ with a deviation from stoichiometry in the direction of Cu_2S and $0.9{\cdot}CuInP_2S_6$ - $0.1{\cdot}In_2S_3$ in the In_2S_3 side, which involves the enrichment of the resulting crystals with copper and indium, respectively. The degree of perfection of the studied crystals can be judged by the shape and maximum value of the dielectric anomaly during the ferroelectric phase transition. We conducted studies of the dielectric properties of crystals obtained by the Bridgman method in comparison with those ones obtained by CTR from the charge of the above-mentioned compositions.

The studied samples were in the form of thin plates with a thickness from 0.05 mm to 0.3 mm and an area of $S \sim 3{\times}3$ mm^2 for crystals grown by the CTR method and a

thickness of about 1 mm and an area of $S \sim 5\times5$ mm^2 for crystals obtained by directed crystallization from the melt. For dielectric measurements, electrodes made of indium-gallium amalgam were applied to large sample planes (perpendicular to the layers), obtained by mechanical chipping. In the frequency range of 100 Hz - 10 kHz, measurements were made by using an LCR-819 LCR-meter.

A sharp jump in ε' upon heating, due to a phase transition of the first kind, in a crystal that was obtained by the CTR method from a charge of stoichiometric composition, is observed at a temperature of 311.3 K, which is very close to the value of T_c, in a crystal grown by the Bridgman method at 312.0 K (Figure 5(*a*)). The peaks of ε'(T) practically coincide in temperature in both types of crystals. The temperature hysteresis of the phase transition for both samples was ~1 K.

In the entire temperature range, a dielectric dispersion is observed, which stretches in a very wide frequency range - from 10^5 Hz to the lowest measured frequencies. Obviously, this dispersion continues even at lower frequencies, since there is a steady tendency to increase ε' and ε" with decreasing frequency. After application to a "fresh" sample of the measured field, its capacitance and dielectric losses have a long-term relaxation. In addition, at temperatures above the ε'(T) jump, the measured dielectric parameters at frequencies below 1kHz depend significantly on the magnitude of the measured field: they increase with the increase of the measured field. At the same time, a sudden increase in the measured field is accompanied by a long-term increase in the measured values of the capacity and tgδ of the sample. These facts indicate the contribution to the low-frequency dielectric response of the volume-charged polarization mechanism due to the presence of electrodes or macroscopic inhomogeneities of the sample. Another explanation for this phenomenon can be due to the ionic contribution to the conductivity of the sample, which increases with increasing temperature. During long-term application of a constant electric field to the $CuInP_2S_6$ sample, one of the electrodes peels off, and copper oxide is observed on its surface. The ionic conductivity of $CuInP_2S_6$, and $CuCrP_2S_6$ crystals was studied in detail in work [31], and is explained by the jump conductivity of Cu+ ions.

The temperature dependences of the real ε' and imaginary ε" parts of the dielectric constant for crystals obtained from a charge with different degrees of stoichiometry are shown in Figure 5. The measurements were performed at a frequency of 100 kHz, at which the low-frequency dielectric response associated with conductivity is practically unaffected by the measurement results in the vicinity of the phase transition. In the crystals obtained from the charge enriched with indium sulfide, the phase transition is shifted to the region of higher temperatures (T_c = 319.8K) in relation to the crystal obtained from the charge of stoichiometric composition. At the same time, in a crystal grown from a charge with an excess of copper sulfide, the phase transition is observed at lower temperatures T_c = 305.3 K. The maximum dielectric constant in this crystal is much higher and the shape of the anomaly is "sharper". In the sample obtained at a high concentration of the CuJ carrier, the phase transition occurs at almost the same temperature as in the crystals grown from the Cu_2S-enriched charge. However, it should be noted that the ε'(T) peak in this sample is more blurred.

The degree of blurring of the dielectric constant anomaly can be seen more clearly from the temperature dependences of 1/ε'(T) (Figure 5(*b*)). For samples obtained from a stoichiometric charge and enriched with Cu_2S, the dependence 1/ε '(T) in a wide temperature range obeys a linear law with the Curie-Weiss constant $C \approx 6.6\times10^3$ K^{-1}. Deviation from the Curie-Weiss law occurs in the range of several K above T_c. In a sample obtained from a charge with an excess of indium sulfide, the Curie-Weiss constant is $C \approx 4.5\times10^3$ K^{-1}. This value is close to the value $C \approx 4.7\times10^3$ K^{-1} obtained for these crystals in [32]. Judging by the degree of blurring of the dielectric anomaly, its temperature position, and the maximum value of ε in the $CuInP_2S_6$ crystal grown from the melt, it can be concluded that these crystals can be compared in terms of quality with crystals obtained from the gas phase from a charge of stoichiometric composition.

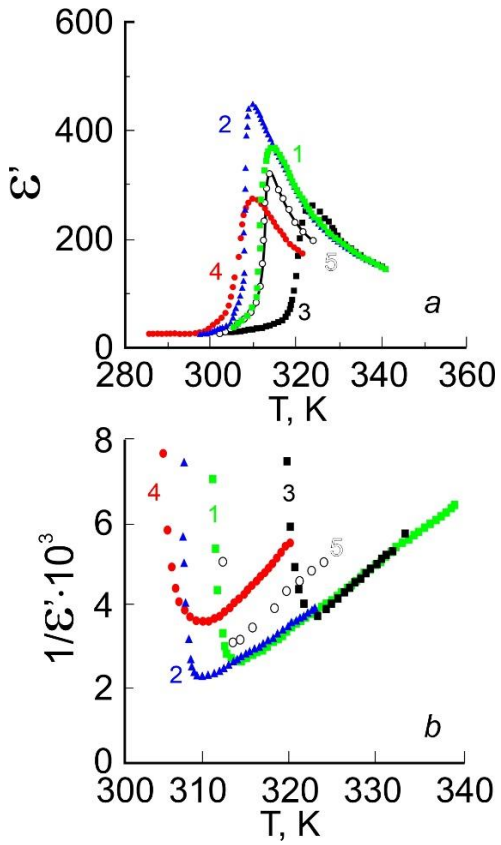

Figure 5. Temperature dependences of ε' and 1/ε' for crystals grown: 1 - from a stoichiometric composition, 2 - from a composition $0.9\cdot CuInP_2S_6$-$0.1\cdot Cu_2S$; 3 - from a composition of $0.9\cdot CuInP_2S_6$ - $0.1\cdot In_2S_3$; 4 - from a stoichiometric composition at a concentration of the transport agent CuJ of 20 mg/cm^3; 5 - by the method of directed crystallization (heating).

Based on the above results, it is possible to qualitatively explain the dependence of the temperature of the phase transition in $CuInP_2S_6$ crystals on the degree of their stoichiometry. The fact that the phase transition occurs at higher temperatures and the dielectric constant anomaly is greater in crystals obtained with an excess of Cu_2S indicates that, most likely, there are copper vacancies in the crystals grown from the stoichiometric composition. In the crystals obtained from the charge with an excess of In_2S_3, apparently, the degree of non-stoichiometry with respect to copper increases even more. Thus, it can be assumed that

with an excess of copper sulfide in the initial raw material for crystal growth, the obtained crystals have a more perfect structure. Conversely, an increase in the content of indium sulfide in the charge leads to an increase in the concentration of crystal lattice defects, namely copper vacancies. As for the case of crystals obtained at high concentrations of the transporting agent (curves 4 in Figure 5(*a*)), it is obvious that the situation here is the same as in the case of samples obtained from a charge enriched with Cu_2S: due to the excess copper contained in the transporting agent, "healing" of copper vacancies takes place. The blurring of the phase transition is probably associated with the introduction of iodine into the interlayer space. As a result, the crystals take on an orange color.

Based on the fact that the occurrence of ferroelectric polarization in $CuInP_2S_6$ is mainly caused by the difference in the occupancy of two non-equivalent non-central positions in the crystal lattice by copper ions [33], copper vacancies can be considered as soft defects that can reorient, and which, as is known [34], shift the phase transition to the region of higher temperatures. Such a qualitative conclusion is well consistent with the situation observed in the experiment.

VI. MULTITYPE ENERGY CONVERTER

We propose to use layered $CuInP_2S_6$ crystals as an active substance for the transducer of deformation, lighting, and heat into electric current. In contrast to the converter, which we implemented earlier [1] based on a composite using 3D ferroelectrics $Sn_2P_2S_6$, the use of layered $CuInP_2S_6$ crystals provides many advantages. First, its photoelectric sensitivity, as shown earlier, is two to three times higher than in the case of $Sn_2P_2S_6$. In addition, there is no need to orient the crystals when applied to the supporting electrode, due to the spontaneous polarization in them is directed perpendicular to the layers. By reason of the layered van-der-Waals nature of $CuInP_2S_6$ crystals, it is much easier to create thin-layer and ultra-thin-layer converters. In the case of $Sn_2P_2S_6$, the layer thickness was limited by the minimum size of microcrystals (~50 μm), below which the ferroelectricity phenomenon disappears in them.

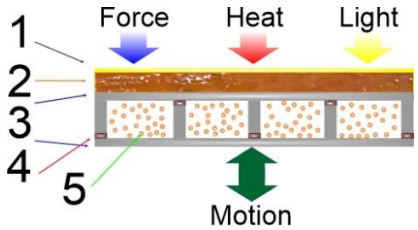

Figure 6. Schematic section of the converter of deformation, lighting, heat and motion into electric current.

The design of the converter proposed by us is very simple and is shown in Figure 6. The active single-crystal layer 2 of the $CuInP_2S_6$ crystal is placed between the translucent electrode 1 (sputtered thin layer of gold or stanum oxide) and the main carrier electrode 3 made of thin (1 mm) aluminum. This sandwich structure, due to the ferroelectric properties of the active material, converts deformation or compression (due to the piezoelectric effect), illumination (due to the photovoltaic effect), and temperature change (due to the pyroelectric effect) into an electric current, all at the same time.

The lower part of the transducer, consisting of aluminum electrodes 3, flexible rubber insulators 4, and active substance ($Sn_2P_2S_6$ powder) 5, remained practically unchanged [1], not counting the shape of electrodes 3, which, due to 3D architecture, were able to use movement not only in vertical but also in the horizontal direction. This part of the transducer uses the triboelectric [35] and piezoelectric effects to convert motion or vibration into electrical current.

TABLE 2.
COMPARISON OF THE MAIN CHARACTERISTICS OF $CuInP_2S_6$ AND $Sn_2P_2S_6$ SINGLE CRYSTALS

Parameter	$CuInP_2S_6$	$Sn_2P_2S_6$
Tc, °C	42	65
E_g, eV	2.85	2.5
Spontaneous polarization, Ps, μC/cm^2	4	14
ε at 300K	30	280
Piezoelectric coefficient, d_{33}, pm/V	17.4	28.2 ± 1.2
Pyroelectric coefficient, γ, μC/ K m^2	735	750

The operation of this cascade is based on the movement of particles of the active powder (as in a liquid) [1], its friction on the electrodes and particles on each other, and the formation of a charge on the particles of the active substance due to the triboelectric and piezoelectric effect, and its transfer between the electrodes. In this cascade, it is better to use 3D $Sn_2P_2S_6$ crystals as an active substance, in which both the dielectric constant and the piezoelectric coefficient are higher compared to $CuInP_2S_6$. The effect of rapid destruction of active particles with the formation of a parasitic blocking layer on the electrodes described in [28] is proposed to be eliminated by applying a solid protective Al_2O_3 [36] layer on the $Sn_2P_2S_6$ micro crystallites. The parameters of this layer are given in the work [1] and has an output voltage of 180-200V.

With a slight modification of this design, namely by adding a multilayer structure based on $Li_2FeP_2S_6$, $Li_2NiP_2S_6$ [23,24] or SnP_2S_6 [37], we can also add an energy storage device or battery which will make it possible not only to generate but also to store the created energy.

Because different cascades of this converter have different output voltages, namely, the upper cascade is hundreds of millivolts and the triboelectric cascade is hundreds of volts, it is necessary to use special energy harvesting circuits, for example, Analog Devices LTC3330, ADP5092, STMicroelectronics SPV1050 and others [35].

VII. CONCLUSION

Based on the studies carried out, we can conclude that using 2D and 3D ferroelectric and superionic crystals it is possible to create multilayer structures capable of simultaneously converting illumination, deformation, heat, and motion into electricity with its subsequent accumulation. Using layered ferroelectric crystals $CuInP_2S_6$ we can easily create multifunctional transducers of submicron thickness. To increase the operating temperature range, crystals obtained with a stoichiometry deviation, namely, those enriched with indium are most suitable.

ACKNOWLEDGMENT

This work was partially supported by the Hungarian Academy of Sciences Domus Senior Grant No: 87/31/2022/HTMT.

REFERENCES

[1] A. Molnar, D. Gal, H. Ban and V. Gerasimov, "Ferroelectric Based Multi-Type Energy-Harvesting Device to Power a Mobile Medical Telemetry System," *Integrated Ferroelectrics*. Vol.220:1, pp.110-119, 2021.

[2] D. Maurya, A. Pramanick, D. Viehland, *Ferroelectric Materials for Energy Harvesting and Storage*, Woodhead Publishing: Elsevier Ltd., 2021, 647p.

[3] H. Huang, J. F. Scott *Ferroelectric Materials for Energy Applications*, Wiley-VCH, 2018, 376p.

[4] A. Cano, D. Meier, M. Trassin, *Multiferroics: Fundamentals and Applications*, De GRUYTER, 2021, 434p.

[5] K. Uchino *Ferroelectric Devices: 2nd ed.*, Taylor & Francis Group, LLC., 2010, 361p.

[6] X. K. Wei, N. Domingo, Y. Sun, N. Balke, R. E. Dunin-Borkowski, J. Mayer, "Progress on Emerging Ferroelectric Materials for Energy Harvesting, Storage and Conversion," *Advanced Energy Matererials*, Vol.12, p.2201199(22), 2022.

[7] T. Y. Kim, S. K. Kim, "Application of ferroelectric materials for improving output power of energy harvesters," *Nano Convergence*, Vol.5, p.30, 2018.

[8] C. R. Bowen, H. A. Kim, P. M. Weaver, S. Dunn, "Piezoelectric and ferroelectric materials and structures for energy harvesting applications," *Energy Environ. Sci.*, Vol.7, I.1, p.25-44, 2014.

[9] S. Sahoo, T. Vijayakanth, P. Kothavade, P. Dixit, J. K. Zareba, K. Shanmuganathan, R. Boomishankar, "Ferroelectricity and Piezoelectric Energy Harvesting of Hybrid A_2BX_4-Type Halogenocuprates Stabilized by Phosphonium Cations," *ACS Mater. Au*, Vol.2, I.2, p.124–131, 2022.

[10] J. Roscow, Y. Zhang, J. Taylor, C. R. Bowen, "Porous ferroelectrics for energy harvesting applications," *The European Physical Journal Special Topics*, Vol.224, p.2949–2966, 2015.

[11] M. A. Susner, M. Chyasnavichyus, M. A. McGuire, P. Ganesh, P. Maksymovych, "Metal Thio- and Selenophosphates as Multifunctional van der Waals Layered Materials," *Advanced Materials*, Vol.29, I.38, p.1602852(39), 2017.

[12] Б. М. Воронин, Г. П. Приходько, С. А. Кириллов, *Слоистые соединения в системах металл-фосфор-халькоген*, Киев: Наукова думка, 1992, 208с.

[13] K. Z. Rushchanskii, R. M. Bilanych, A. A. Molnar, J. Banys, Y. M. Vysochanskii, "Ferroelectricity in $(Pb_ySn_{1-y})_2P_2S_6$ mixed crystals and random field BEG model," *Physica Status Solidi (B) Basic Research*, Vol.253(2), pp.384–391, 2016.

[14] A. A. Grabar, I. V. Kedyk, M. I. Gurzan, I. M. Stoika, A. A. Molnar, Yu. M. Vysochanskii, "Enhanced photorefractive properties of modified $Sn_2P_2S_6$," *Optics Communications*, Vol. 188, pp.187–194, 2001.

[15] Yu. Tyagur, L. Burianova, I. Tyagur, A. Kopal, P. Hana "The Investigation of Dynamic Piezoelectric Properties of $Sn_2P_2S_6$ Single Crystals," *Ferroelectrics*, Vol.300, pp.165-171, 2004.

[16] J. Song, J. Wang, "Ferroelectric materials for vibrational energy harvesting," *Science China Technological Sciences*, Vol.59, I.7, pp.1012–1022, 2016.

[17] M. M. Maior, M. I. Gurzan, Sh. B. Molnar, I. P. Prits, Yu. M. Vysochanskii, "Effect of germanium doping on pyroelectric and piezoelectric properties of $Sn_2P_2S_6$ single crystal," *IEEE Transactions on Ultrasonics, Ferroelectrics, and Frequency Control*, Vol.47, I.4, pp.877–880, 2000.

[18] A. P. Sharma, M. K. Behera, D. K.Pradhan et al. "Lead-free relaxor-ferroelectric thin films for energy harvesting from low-grade waste-heat," *Scientific Reports*, Vol.11, p.111, 2021.

[19] P. Kulkarni, S.K. Nataraj, R.G. Balakrishna, D.H. Nagaraju, M.V. Reddy, "Nanostructured binary and ternary metal sulfides: synthesis methods and their application in energy conversion and storage devices," *Journal of Materials Chemistry A.*, Vol. 5, pp. 22040–22094, 2017.

[20] S. Mengwei, P.Y. Liao, G. Qiu, Yu. Duan, P.D. Ye, "Ferroelectric Field-Effect Transistors Based on MoS_2 and $CuInP_2S_6$ Two-Dimensional Van der Waals Heterostructure," *ACS Nano*, Vol. 12, I. 7, pp.6700-6705, 2018.

[21] К. А. Воротилов, В. М. Мухортов, А. С. Сигов, *Интегрированные сегнетоэлектрические устройства*, Москва: Энергоатомиздат, 2011, 175 с.

[22] L. Fucai, Yo. Lu, K. L. Seyler, L. Xiaobao, Yu. Peng, L. Junhao at. al, "Room-temperature ferroelectricity in $CuInP_2S_6$ ultrathin flakes," *Nature Communications*, Vol. 7, p.12357(6), 2016.

[23] K. Takada, Y. Michiue, T. Inada, A. Kajiyama, M. Kouguchi, S. Kondo at. al, "Lithium iron thio-phosphate: a new 3 V sulfide cathode," *Solid State Ionics.* Vol. 159, pp.257–263, 2003.

[24] P. J. S. Foot, T. Katz, S. N. Patel, B. A. Nevett, A. R. Piercy, A. A. Balchin, "The Structures and Conduction Mechanisms of Lithium-Intercalated and Lithium-Substituted Nickel Phosphorus Trisulphide ($NiPS_3$), and the Use of the Material as a Secondary Battery Electrode," *Physica Status Solidi (a)*, Vol. 100, pp.11-29, 1987.

[25] J. Banys, A. Dziaugys, K. E. Glukhov, A. N. Morozovska, N. V. Morozovsky, Yu. M. Vysochanskii, *Van der Waals Ferroelectrics: Properties and Device Applications of Phosphorous Chalcogenides*, Wiley-VCH, 2022, 395p.

[26] И. П. Приц, М. М. Майор, Ю. М. Высочанский, А. А. Молнар, М. И. Гурзан, Н. Ф. Корда, "Получение монокристаллов гексатиогиподифосфата $CuInP_2S_6$ методами ХТР и направленной кристаллизации из расплава и их сегнетоэлектрические свойства," *Материалы восьмого Международного симпозиума «Высокочистые металлические и полупроводниковые материалы»*, Харьковь, с.103-105, 2002.

[27] H. Bán, D. Gal, V. Gerasimov, A. Haysak, A. Molnar, "Automated measuring system for studying the temperature dependence of dielectric spectra of ferroelectrics," *IDAACS 2021 The 11th IEEE International Conference on Intelligent Data Acquisition and Advanced Computing Systems: Technology and Applications*, Cracow, Poland, pp.156-159, September 2021.

[28] Yu. M. Vysochanskii, A. A. Molnar, A. A. Gorvat, Yu. S. Nakonechnii, "Phase transitions in the vicinity of lifshitz point in ferroelectrics-semiconductors," *Ferroelectrics*, Vol.169(1), pp. 141–148, 1995.

[29] V. S. Shusta, I. P. Prits, P. P. Guranich, E. I. Gerzanich, A. G. Slivka, "Dielectric properties of $CuInP_2S_6$ crystals under high pressure," *Condensed Matter Physics*, Vol. 10, pp.91–94, 2007.

[30] M. A. Susner, M. Chyasnavichyus, A. A. Puretzky, Q. He, B. S. Conner, Y. Ren, at. al, "Cation−Eutectic Transition via Sublattice Melting in $CuInP_2S_6/In_{4/3}P_2S_6$ van der Waals Layered Crystals," *ACS Nano*, Vol.11, pp.7060−7073, 2017.

[31] V. Maisonneuve, J. M. Reau, M. Dong, V. B. Cajipe, C. Payen, J. Ravez, "Ionic conductivity in ferroic $CuInP_2S_6$ and $CuCrP_2S_6$," *Ferroelectrics*, Vol. 196, pp.257-260, 1997.

[32] A. Simon, J. Ravez, V. Maisonneuve, C. Payen, V. B. Cajipe, "Paraelectric-Ferroelectric Transition in the Lamellar Thiophosphate $CuInP_2S_6$," *Chemistry of Materials*, Vol. 6, pp. 1575-1580, 1994.

[33] V. Maisonneuve, M. Evain, C. Payen, V.B. Cajipe, P. Molinié, "Room-temperature crystal structure of the layered phase $Cu^{I}In^{III}P_2S_6$," *Journal of Alloys and Compounds*, Vol. 218, pp.157-164, 1995.

[34] А. Брус, Р. Каули, *Струтурные фазовые переходы*, Москва:Мир, 1984, 407с.

[35] O. Molnar, V. Gerasimov, I. P. Kurytnik, "Triboelectricity and construction of power generators based on it," *Przegląd Elektrotechniczny*, N.1, pp.167-171, 2018.

[36] M. D. Groner, F. H. Fabreguette, J. W. Elam, S. M. George, "Low-Temperature Al_2O_3 Atomic Layer Deposition," *Chem. Mater.*, Vol.16, pp.639-645, 2004.

[37] J. Hu, A. Zheng, E. Pan, J. Chen, R. Bian, J. Li, at. al, "2D semiconductor SnP_2S_6 as a new dielectric material for 2D electronics," *Journal of Materials Chemistry C.*, pp.2050-7526, 2022.

AUTHOR INDEX